Original Article

Institution of MECHANICAL ENGINEERS
Journal of ENGINEERING IN MEDICINE

Proc IMechE Part H:
J Engineering in Medicine
226(4) 320–329

DOI: 10.1177/0954411912438038
pih.sagepub.com
SAGE

Biomechanical measurements of axial crush injury to the distal condyles of human and synthetic femurs

Meghan Crookshank[1,2], Jason Coquim[3], Michael Olsen[1,2], Emil H Schemitsch[1,2], Habiba Bougherara[3] and Rad Zdero[2,3]

Abstract

Few studies have evaluated the 'bulk' mechanical properties of human longbones and even fewer have compared human tissue to the synthetic longbones increasingly being used by researchers. Distal femur fractures, for example, comprise about 6% of all femur fractures, but the mechanical properties of the distal condyles of intact human and synthetic femurs have not been well quantified in the literature. To this end, the distal portions of a series of 16 human fresh-frozen femurs and six synthetic femurs were prepared identically for mechanical testing. Using a flat metal plate, an axial 'crush' force was applied in-line with the long axis of the femurs. The two femur groups were statistically compared and values correlated to age, size, and bone quality. Results yielded the following: crush stiffness (human, 1545 ± 728 N/mm; synthetic, 3063 ± 1243 N/mm; $p = 0.002$); crush strength (human, 10.3 ± 3.1 kN; synthetic, 12.9 ± 1.7 kN; $p = 0.074$); crush displacement (human, 6.1 ± 1.8 mm; synthetic, 2.8 ± 0.3 mm; $p = 0.000$); and crush energy (human, 34.8 ± 15.9 J; synthetic, 18.1 ± 5.7 J; $p = 0.023$). For the human femurs, there were poor correlations between mechanical properties versus age, size, and bone quality ($R^2 \leqslant 0.18$), with the exception of crush strength versus bone mineral density ($R^2 = 0.33$) and T-score ($R^2 = 0.25$). Human femurs failed mostly by condyle 'roll back' buckling (15 of 16 cases) and/or unicondylar or bicondylar fracture (7 of 16 cases), while synthetic femurs all failed by wedging apart of the condyles resulting in either fully or partially displaced condylar fractures (6 of 6 cases). These findings have practical implications on the use of a flat plate load applicator to reproduce real-life clinical failure modes of human femurs and the appropriate use of synthetic femurs. To the authors' knowledge, this is the first study to have done such an assessment on human and synthetic femurs.

Keywords

Biomechanics, injury, femurs, human, synthetic, condyles

Date received: 7 May 2011; accepted: 16 January 2012

Introduction

Human bone fractures are one of the most common causes of hospitalization with 1.1 million treatments each year in the US, many of which involve the femur.[1] Distal femur fractures make up about 6% of all femur fractures, with 61% of distal femur injuries occurring in young men about 20 years of age involved in motor vehicle accidents or sporting mishaps, and 33% occurring in osteoporotic women about 70 years of age owing to a fall at home.[2,3]

Distal femur fractures are classified as either extra-articular fractures located above the condyles themselves (type A), unicondylar fractures involving one condyle (type B), or bicondylar fractures involving both condyles (type C).[4,5] These are further subdivided according to the degree of comminution of the metaphysis or the articular surface. Surgical treatments for this injury pattern employ extramedullary plates or intramedullary nails that are mounted using cortical screws and sometimes supplemented with bone grafting, although total knee replacement is an option for osteoporotic patients

[1]Faculty of Medicine, University of Toronto, Canada
[2]Martin Orthopaedic Biomechanics Laboratory, St Michael's Hospital, Canada
[3]Department of Mechanical and Industrial Engineering, Ryerson University, Canada

Corresponding author:
Rad Zdero, Biomechanics Laboratory, St Michael's Hospital, Li Ka Shing Institute, 38 Shuter Street, Toronto, ON, M5B-1W8, Canada.
Email: zderor@smh.ca

with poor fracture healing capacity.[3,5] Unsuccessful surgery can result in non-union requiring further bone grafting and stabilization, malunion necessitating corrective osteotomy, arthrofibrosis requiring aggressive rehabilitation and potential arthrodesis, and post-traumatic arthritis treated with non-steroidal anti-inflammatories.[5] Clinical management of distal femur fractures continues to be a challenge.

Biomechanical studies, therefore, have characterized human and synthetic femurs under various loading conditions in intact or instrumented states.[6–20] These studies have focused on assessing axial, torsional, lateral, three-point bending, and four-point bending stiffness and/or strength. Quasi-static, cyclic, and/or impact loads are applied at the femoral head to simulate hip joint loading during walking and other activities of daily living, or at the midshaft to simulate side loads from accidents or falls. Investigations that have specifically examined distal condylar fractures have usually been performed by fabricating idealized and standardized injury patterns to replicate clinical scenarios.[17–20] These are surgically repaired and mechanically tested to determine which technique or implant provides the greatest mechanical stability. However, to the authors' knowledge, no researchers to date have quantified the actual mechanism involved in causing the initial injury to the distal condylar region of intact human versus synthetic femurs.

Consequently, the present aim was two-fold. First, the authors wanted to quantify the stiffness and strength parameters during 'crush injury' from an axial force to the distal condyles of a series of human and synthetic femurs. Second, the authors wanted to determine whether a simple flat plate load application system could simulate real-life clinical injury mechanisms that occur during 'dashboard' injuries in motor vehicle accidents, 'knee first' high-energy sports trauma, and 'knee first' low-energy falls in the elderly. It was hypothesized that human and synthetic femurs would display similar mechanical results. This is the first report in the literature to do so.

Methods

General approach

The distal condyles of a series of human cadaveric and synthetic femurs were subjected to 'crush' injury by the application of an axial force using a metal flat plate. The question was whether or not this could simulate real-life distal condylar fracture patterns owing to 'dashboard' motor vehicle accidents, 'knee first' sports injuries, and 'knee first' accidental falls of the elderly. Synthetic femurs were used because of their increasing prevalence in biomechanical studies, necessitating a need to validate them against the 'gold standard' of human cadaveric femurs for this clinically important injury.

Femur specifications

Sixteen fresh frozen human cadaveric specimens were obtained by permission of the authors' institutional research ethics board. Femurs were stripped of soft tissue as much as possible and visually inspected to ensure no bony pathology. Donor medical histories, if available, were consulted to confirm the absence of bony pathology, which was not found. Femurs were thawed at room temperature for 12 h before preparation and mechanical testing. Demographic, geometric, and bone quality characteristics for the human femurs were recorded (Table 1).

Table 1. Demographic, geometric, and bone quality characteristics of human femurs. Bone quality was classified according to clinical T-scores: $T < -2.5$, osteoporotic; $-2.5 < T < -1.0$, osteopenic; $T > -1.0$, normal.

Human femur characteristics								
Bone	Side	Sex	Age (yrs)	AP condylar width (mm)	ML condylar width (mm)	sBMD (g/cm^2)	T-score	Bone quality
1	L	F	87	67.2	84.1	0.902	−0.8	Normal
2	L	F	73	66.4	84.2	0.927	−0.6	Normal
3	L	M	93	68.2	86.2	0.843	−1.9	Osteopenic
4	L	M	55	69.2	87.8	1.013	−0.6	Normal
5	L	F	79	64.6	83.6	0.999	0.0	Normal
6	L	F	48	61.9	72.0	1.196	1.6	Normal
7	L	M	67	69.2	86.8	1.163	0.6	Normal
8	L	F	75	57.1	73.0	0.638	−3.0	Osteoporotic
9	L	F	45	62.0	71.7	1.193	1.6	Normal
10	L	M	81	69.6	89.7	1.022	−0.5	Normal
11	L	F	72	65.5	89.7	0.917	−0.7	Normal
12	L	F	79	63.3	79.3	0.669	−2.8	Osteoporotic
13	L	F	80	70.0	84.3	0.866	−1.1	Osteopenic
14	L	F	43	69.8	84.6	1.196	1.6	Normal
15	L	F	62	67.5	88.4	1.042	0.3	Normal
16	L	F	70	73.3	86.2	0.952	−0.4	Normal
AVG			69.3	66.6	83.2	0.971	−0.4	Normal
SD			14.9	4.0	6.0	0.171	1.4	—

AP: anteroposterior; AVG: average; ML: mediolateral; sBMD: standardized bone mineral density; L: left; F: female; M: male; SD: standard deviation.

Six large, left, fourth-generation composite femurs (Model #3406, Pacific Research Laboratories, Vashon, WA, USA) were 'off the shelf' from the manufacturer and had a simulated cortical bone density of 1.64 g/cm^3, a simulated cancellous bone density of 0.32 g/cm^3 ('cellular' matrix), an intramedullary canal diameter of 16 mm, an anteroposterior condyle width of 67 mm, and a mediolateral condyle width of 92 mm. The artificial bone density values were within the range for human cortical (1.6–2.1 g/cm^3) and human cancellous (0.1–1.0 g/cm^3) bone.[21,22]

Bone mineral density

Using the Prodigy^{TM} system and enCORE software 8.80 (Lunar Corp., Madison, WI, USA), dual energy x-ray absorptiometry (DEXA) scans were performed of the femur neck, Ward's region, and trochanter to obtain total bone mineral density (BMD) measurements of the human femurs. For the Prodigy^{TM} system, the weight and height of donors are typically used to define the scan mode, though this did not make any difference presently, since body fat and muscle were absent; thus, the standard scan mode was used. Rice bags were employed as surrogates of surrounding tissue to minimize any measurement artifact. DEXA values from this machine were converted to standardized BMD (sBMD) and clinical T-scores to allow for inter-study comparison.

Femur preparation

Using an industrial band saw, all human and synthetic femurs had their distal 165 mm segment removed. The distal segment was then mounted upside-down onto a chemistry stand using an adjustable multi-axial clamp. The distal shaft was lowered and inserted into the center of a hollow square-channel steel potting chamber (88 mm wide × 88 mm wide × 80 mm high). Using leveling gauges placed at the same anterior location of each femur, the posterior surface of the distal shaft was aligned vertically. To ensure that the flat load application plate to be used later would engage both condyles simultaneously, it was important that the top of the condyles was horizontal. This was done by placing a thin metal plate on top of the condyles, placing a leveling gauge on top of this plate, and then adjusting the orientation of the femur until the leveling gauge indicated the plate was perfectly horizontal. Anchoring cement (Flow-Stone, King Packaged Materials Company, Burlington, ON, Canada) was then mixed according to the manufacturer's instructions and poured into the steel potting chambers until they were filled to the brim. The cement was allowed to dry at least 1 h prior to specimen removal from the clamping system. The resulting working lengths of all femoral specimens from the top of the steel potting chambers to the top of the femoral condyles were identical (85 mm).

Mechanical testing

The specimens were mounted into an industrial clamping system with the femoral condyles facing up (Figure 1). A vertical preload of 100 N was introduced by a metal flat plate onto both condyles simultaneously to reduce any mechanical 'slack', i.e. hysteresis, in the setup. An unpadded flat metal plate was used for load application onto the femoral condyles. This was similar to two prior reports that used unpadded flat metal plates, one study that tested human knees with the patella intact and another study that tested femoral condyles without mimicking tibial condyles or the patella.[23,24] Using displacement control at a constant rate of 5 mm/min, a vertical force was applied through the metal flat plate to both condyles simultaneously until there was complete structural collapse of the specimen. A fixed low speed for load application was chosen in order to standardize the procedure for all specimens and to minimize any time-related viscoelastic effects. Moreover, the advantage of using a low speed, rather than an impact load to simulate motor vehicle accidents and sports injuries, was that the study would provide a lower bound value for the measurements.

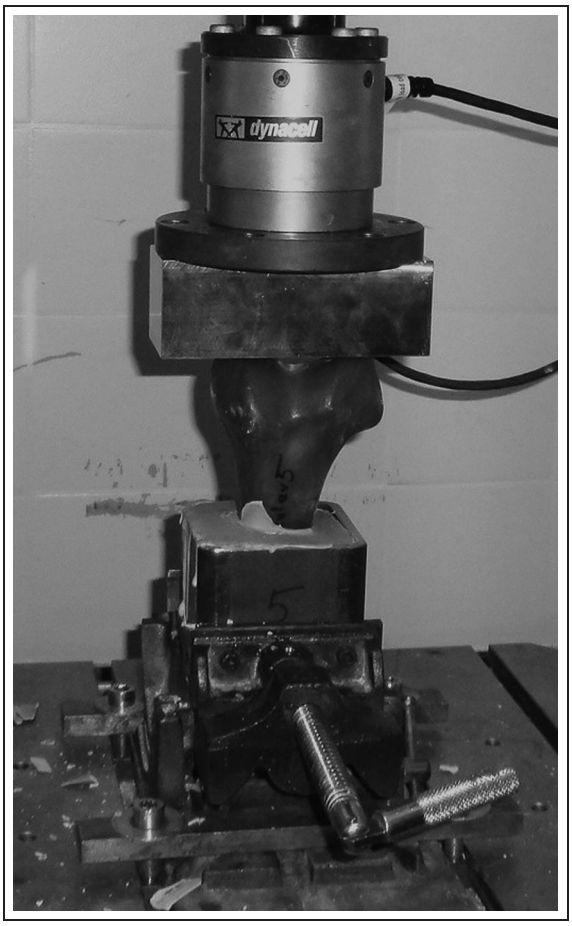

Figure 1. Experimental setup showing (from top to bottom) the load cell, vertical force application plate, upside-down femur, cement potting steel cube, and industrial clamp. Human and synthetic femurs were tested using this identical configuration.

Table 2. Comparison of human versus synthetic femur results for mechanical properties. Values given are averages with standard deviations in parentheses. A statistically significant difference was noted for $p < 0.05$.

Mechanical property	Human femurs	Synthetic femurs	*p*-value
Crush stiffness (N/mm)	1545 (728)	3063 (1243)	0.002
Crush strength (N)	10,334 (3093)	12,861 (1651)	0.074
Crush displacement (mm)	6.1 (1.8)	2.8 (0.3)	0.000
Crush energy (J)	34.8 (15.9)	18.1 (5.7)	0.023

The use of a non-impact loading speed (6 mm/min) has also been used in a prior similar, but much smaller, study on 6 human femurs.[24] Present experiments were performed at ambient room temperature. An Instron 8874 machine (Instron, Norwood, MA, USA) was used for all mechanical tests. The load cell had a capacity of ± 25 kN, a resolution of 0.1 N, and an accuracy of ± 0.5%. The tester had an axial stiffness of 260 kN/mm, which is about 340 and 200 times stiffer, respectively, than typical intact human and synthetic femurs,[6] thereby requiring no adjustments to the results to accommodate for machine compliance.

Data collection

All data were collected at an Instron software sampling rate of 10 Hz, i.e. 0.1 s intervals. A force-versus-displacement graph was generated for each specimen during 'crush injury' from which crush stiffness (i.e. slope of the linear portion of the curve up to 1000 N), crush strength (i.e. peak force), crush displacement (i.e. vertical displacement corresponding to the peak force), and crush energy (i.e. area under the curve up to and including the peak force) were extracted. Stiffness values extracted involved only the linear elastic portion of the force-versus-displacement graphs, yielding average linearity values of $R^2 = 0.99$ (human femurs) and $R^2 = 1.00$ (synthetic femurs).

Statistical analysis

Statistical comparisons between femur groups were done with Microsoft Office Excel 1997–2003 (Microsoft Corp., Redmond, WA, USA) using the single one-way analysis of variance (ANOVA) function. Statistical significance was set at $p < 0.05$. Human femur age, anteroposterior condylar width, mediolateral condylar width, and bone quality were correlated to the measured parameters using the coefficient R^2. A one-tailed post hoc power analysis was performed using an alpha level of 5%, i.e. 95% confidence interval, to determine if there were enough specimens per group to permit the detection of all statistical differences that may have been actually present, i.e. avoiding type II error. Moreover, after the study, an estimation was made of δ, i.e. the minimum difference between human and synthetic femur groups that could be considered clinically important and/or that was detectable statistically. This was computed using $\delta = (\mu_1 - \mu_2)/\sigma \times [(N_1 \times N_2)/(N_1 + N_2)]^{1/2}$ where μ = average value of the particular measurement for each femur group, σ = total population standard deviation = 3, and N = number of specimens per femur group.[25,26]

Results

Crush measurement results

Crush measurements for human and synthetic femurs are given (Table 2). Synthetic femurs had a crush stiffness 1.98 times higher than that of human femurs ($p = 0.002$). Synthetic femurs had a crush strength 1.24 times higher than results from human femurs, although the difference was not statistically significant ($p = 0.074$). Human femur crush displacement was 2.18 times higher than for synthetic femurs ($p = 0.000$). Human femur crush energy was 1.92 times higher than values for synthetic femurs ($p = 0.023$).

Crush measurements correlated to age, size, and bone quality

Crush measurements for human femurs were correlated to demographic, geometric, and bone quality parameters (Table 3). Almost all correlations were poor ($0.00 \leqslant R^2 \leqslant 0.18$), indicating no linear predictive relationships existed for these comparisons. The exception was crush strength versus bone quality, either expressed as standardized BMD (sBMD) ($R^2 = 0.33$) or clinical T-score ($R^2 = 0.25$).

Table 3. Correlation coefficient values R^2 indicating the amount of agreement between a straight line of best fit and human femur data. Perfect correlation would yield $R^2 = 1$.

Correlation coefficient, R^2				
Parameter	Crush stiffness	Crush strength	Crush displacement	Crush energy
Age	0.01	0.09	0.11	0.01
AP width	0.00	0.03	0.09	0.06
ML width	0.02	0.05	0.15	0.11
sBMD	0.08	0.33	0.11	0.18
T-score	0.06	0.25	0.06	0.10

AP: anteroposterior; ML: mediolateral; sBMD: standardized bone mineral density.

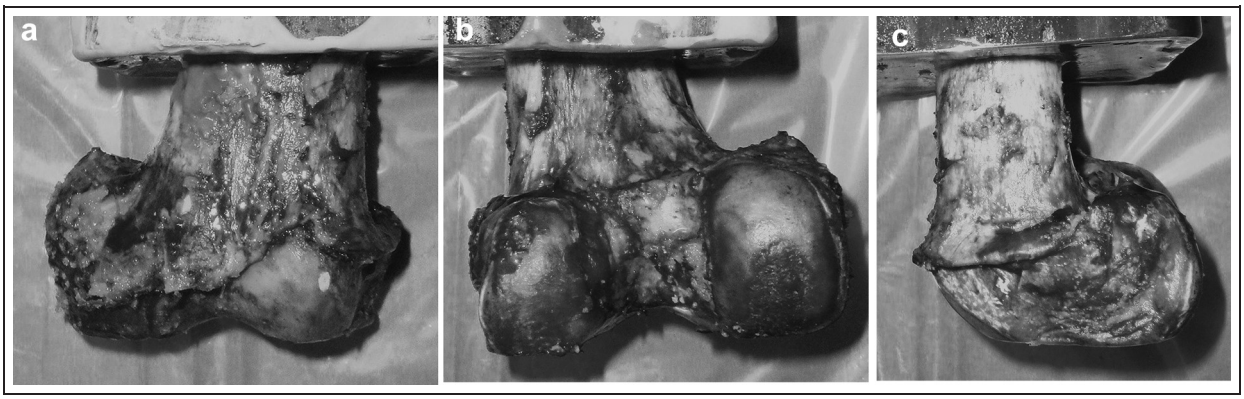

Figure 2. The most common failure mode (15 of 16 cases) for human femurs showed buckling 'roll back' of the condyles against the femur shaft. (a) The anterior surface, (b) the posterior surface, and (c) the lateral surface.

Crush failure mode

Human femurs failed with a variety of simultaneous damage patterns (Figure 2, Table 4). By far, the most common human femur failure mode was condyle buckling by 'roll back' of the condyles against the femur shaft (15 of 16 cases). A number of femurs showed a fracture line in-between the condyles that was parallel to the shaft axis (6 of 16 cases). A few femurs yielded gross failure through the femur shaft by a fracture plane parallel to the long axis (2 of 16 cases). A couple of specimens evidenced a fracture line through the lateral condyle that was parallel to the shaft axis (2 of 16 cases). Several femurs failed at the femur-cement interface (4 of 16 cases). No femurs had fully displaced condylar fractures.

All synthetic femurs failed in a similar manner to one another (Figure 3). Regarding the medial condyle, the anterior surface had a fracture line that started at the exposed intramedullary canal hole, went in-between the condyles, and ended above the medial condyle, resulting in its complete detachment from the femur shaft, i.e. fully displaced fracture (6 of 6 cases). Regarding the lateral condyle, the posterior surface showed that the lateral condyle had a fracture line that was parallel to the femur shaft axis and that may or may not have been accompanied by a fracture line under the condyle itself (5 of 6 cases). This resulted in complete detachment of the lateral condyle from the femur shaft, i.e. fully displaced fracture, in some specimens (3 of 6 cases). All lateral condyles had some damage to the cortical shell starting around the load application point (6 of 6 cases). No femurs had damage at the bone-cement interface, experienced condyle 'roll back' buckling, or translated horizontally under the loading plate.

Table 4. Failure modes for human femurs indicating a combination of 'roll back' of the condyles against the femur shaft (RB), inter-condylar fracture (IC), lateral condyle fracture (LC), femur shaft fracture (FS), and femur-cement interface fracture (FC).

Specimen	Failure mode				
	RB	IC	LC	FS	FC
1	•				
2	•				•
3	•				
4	•				
5	•	•			
6	•		•		•
7	•	•			
8	•	•			
9					•
10	•			•	
11	•				
12	•				•
13	•	•	•		
14	•				
15	•	•		•	
16	•	•			

Post hoc power analysis

To assess the quality of the statistical comparisons of the two femur groups, post hoc power analysis was done and yielded 87.9% (crush stiffness), 79.3% (crush strength), 100.0% (crush displacement), and 97.5% (crush energy). Thus, the average power was 91.2%. A good study design is normally considered to be 80% or higher. This means, for this investigation, that there were enough femurs per test group to detect all the statistical differences that may have been actually present, i.e. type II error was avoided. Moreover, the minimum differences that could be considered clinically important and/or statistically detectable between the two femur groups were 1057 N/mm (crush stiffness), 1760 N (crush strength), 2.3 mm (crush displacement), and 11.6 J (crush energy).

Discussion

General findings

The authors investigated axial crush injury of the distal condyles of both human and synthetic femurs. The two

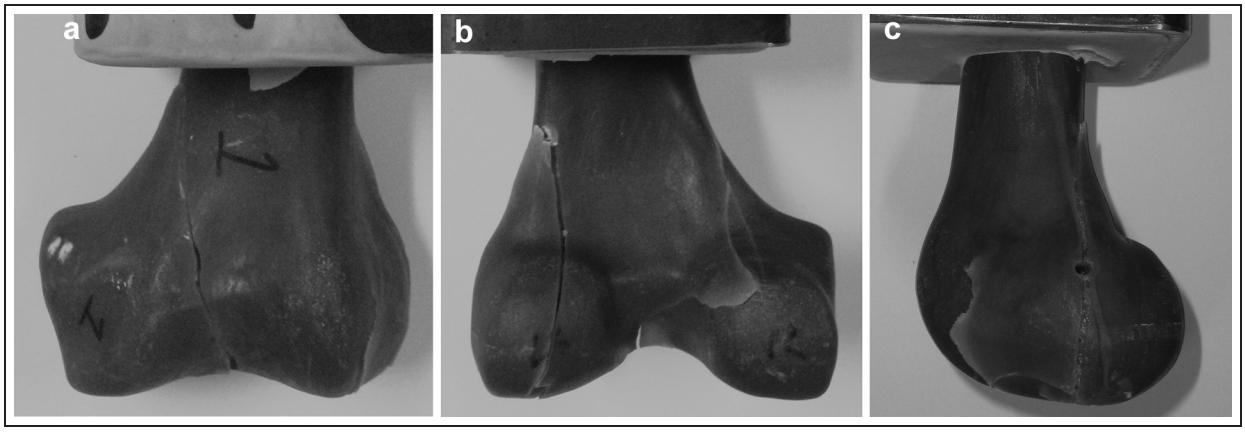

Figure 3. Typical failure mode for the distal condyles of synthetic femurs. (a) The anterior surface had a fracture line running in-between the condyles across the exposed intramedullary canal hole, (b) the posterior surface evidenced a fracture line through the lateral condyle and a fracture line alongside the medial condyle, and (c) the lateral surface showed a crack.

groups of specimens were statistically different for three of four mechanical measurement outcomes. There were poor correlations between mechanical measurements versus human femur age, geometry, and bone quality, with the exception of a moderate correlation between crush strength versus BMD and T-score. In most cases, failure modes were different between human and synthetic femurs. To the authors' knowledge, this is the only study in the literature to have done such an assessment.

Comparison with prior studies

Only a few prior studies have quantified any type of injury to the intact distal human femur[23,24] and none have done so for synthetic femurs. Any differences between current results and those of these previous studies are owing to variations in experimental setup, such as the use of human and/or synthetic femurs, bone quality, load application speed, the presence or absence of surrounding tissue, etc. Thus, direct comparison with present findings may be problematic, although pertinent points can be noted.

Viano and Stalnaker assessed the mechanisms of failure for only six fully intact cadaveric human knee joints and femur shafts by applying impact loads at about 13 m/s using an unpadded rigid metal flat plate with the femur shafts in-line with the axis of impact.[23] They found specimen average stiffness to be 1000 N/mm (range, 600–2000 N/mm) with subsequent fracture initiated at a force of 10.6 ± 2.6 kN, a compression of 13.0 ± 0.7 mm, and an energy of 396 J. They observed that specimen fracture was owing predominantly to anteroposterior shaft bending or patellar wedging in-between the femoral condyles. Similarly, current femur failure loads were 10.3 ± 3.1 kN (human) and 12.9 ± 1.7 kN (synthetic). However, present femur stiffnesses (1545 ± 728 N/mm, human; 3063 ± 1243 N/mm, synthetic), failure displacements (6.1 ± 1.8 mm, human; 2.8 ± 0.3 mm, synthetic), and failure energies (34.8 ± 15.9 J, human; 18.1 ± 15.7 J, synthetic) were substantially different than theirs. In contrast, current human femurs failed mainly by 'roll back' buckling of the condyles (15 of 16 cases), although many specimens did show some type of shaft fracture (6 of 16 cases) or inter-condylar wedging (6 of 16 cases) consistent with the prior study. Present synthetic specimens also showed inter-condylar fracture (6 of 6 cases). No correlation to age, geometry, or bone quality was reported by the previous researchers.

Murray et al. obtained six intact human cadaveric femurs, stripped them of soft tissue, removed the distal 60 to 84 mm portion with the condyles intact, and mounted the specimens into cement potting chambers.[24] They prevented translation of the specimen by using support blocks. Axial forces were applied until failure, but only to the lateral condyle, at a non-impact loading speed of 6 mm/min using a metal flat plate lined with a thin layer of rubber to simulate deformable cartilage. Their average stiffness (1470 ± 404 N/mm) and failure energy (27.3 ± 14.7 J) were quite similar to current human specimens, but their failure force (7782 ± 3024 N) was substantially lower. Similar to the present study, they used an unpadded flat metal plate and applied a non-impact speed for load application. However, in contrast, they used only six specimens, they only loaded the lateral condyle, and they did not report average failure displacement, failure mode, or the degree of correlation with age, geometry, or bone quality.

Practical implications

Synthetic femurs yielded statistically different results compared with human femurs for crush stiffness, but not crush strength. A prior investigation on the same model of intact synthetic femurs showed that even a six-fold increase in its cancellous density only slightly altered axial, lateral, and torsional stiffness, but substantially affected failure load, displacement, and energy.[27] External geometry and cortical properties are

fixed by the synthetic bone's manufacturer, while changes are usually only possible to cancellous matrix density and intramedullary canal diameter. This suggests that future researchers can only seek to modify these latter two parameters if trying to realistically simulate distal human femur failure strength, but they should not expect to accurately mimic distal human femur stiffness.

The relationship between human femur bone quality and crush strength was by far the highest observed among the current study's computed correlations, yielding coefficients of $R^2 = 0.33$ (sBMD) and $R^2 = 0.25$ (T-score), although in absolute terms these were still rather weak correlations. This agrees with other reports showing correlations, albeit stronger, between human BMD versus failure load for femoral hip resurfacings ($R^2 = 0.64$),[28] cortical bone screw pullout force in femoral cortical bone ($R^2 = 0.88$),[29] and cancellous bone screw pullout force in femoral cancellous bone ($R^2 = 0.89$).[30] Moreover, in a prior study on femoral neck fracture in a series of intact synthetic femurs, there was also a clear relationship between cancellous matrix density and axial failure load applied to the femoral head ($R^2 = 0.92$).[27] This shows that bone quality, in general, is highly predictive of the forces required to fail both intact and instrumented femurs and, specifically, may be the most predictive for axial crush injury of the distal condyles of intact human femurs during motor vehicle accidents, sports activities, or falls.

The failure modes of current human femurs suggest the potentially important role of the patella in high-energy 'dashboard' injuries during motor vehicle accidents, 'knee first' sporting mishaps, or 'knee first' falls. This causes the patella to be pushed in-between the condyles, wedging them apart, as noted in one biomechanical study on fully intact human lower limbs.[23] These injuries are clinically classified as unicondylar (type B) or bicondylar (type C) fractures.[4,5] Less than half (7 of 16 cases) of current human femur failures were in this category, most likely because a non-conforming flat metal plate was used for load application that did not simulate patellar wedging. However, a previous study also used this approach.[24] Conversely, all present synthetic femur failures were similar to clinical failures of type B or type C. The stress concentration from the exposed intramedullary canal located in-between the condyles may have predisposed them to wedge-type failure as seen clinically owing to patellar wedging. As such, the present authors have shown experimentally that a simple metal flat plate used to apply load to human specimens usually cannot simulate real-life type B or C clinical failure patterns. Researchers should also be aware that these 'off-the-shelf' synthetic femurs are commercially manufactured with an exposed intramedullary hole and are almost universally used in the biomechanics literature in this form. Thus, any distal femoral fracture patterns reported in the literature using these synthetic bones should be evaluated with this fact in mind.

To better understand the mechanical failure of the distal femurs observed at present, a useful analogy may be axial compression of a column, i.e. Euler column buckling.[31] If the boundary conditions are approximated, such a column could reasonably simulate the current distal femur experiments. First, consider a column free at the top end and rigidly fixed at the bottom end. Second, because of its free end, this column would ideally buckle with a deflection curve in the shape of a half-period sine wave. Third, the applied force is purely axial, i.e. it is parallel to the long axis of the column. Fourth, assume the column is made from a solid piece of isotropic material with uniform material properties in all directions. Fifth, the cross-sectional area of the column is rectangular in shape. The relevant Euler column buckling equations for a free-fixed column can be mathematically reduced to $F_{CR} = (\pi^2 EI)/(16H^2)$, where F_{CR} = critical force required for buckling, E = modulus of elasticity, I = area moment of inertia about the neutral axis, and H = column height. Assume the column has E = 137 MPa, based on the manufacturer's specifications for the synthetic 'cellular matrix' cancellous bone used presently, since it occupies most of the distal femur volume.[32] The moment of inertia for the column can be computed as $I = W_{AP} \times W_{ML}^3/12$, where W_{AP} = average anteroposterior femur width = 66.6 mm and W_{ML} = average mediolateral femur width = 83.2 mm (Table 1). The column height H is based on the working height of the current femurs at 85 mm. Therefore, the predicted square column buckling force F_{CR} = 37 kN. This is about 3 to 3.5 times larger than current experiments. Clearly, this simple and idealized column model is unable to account for the asymmetrical geometry, the composite material properties, and the complex failure mechanisms of a real distal femur. Nonetheless, this column analogy allows for a rudimentary calculation and basic understanding of the mechanism of failure observed in the present specimens. Furthermore, the analogy cannot be used to identify which specific regions of the distal femur are least resistant to failure. More comprehensive mathematical modelling by future researchers of the distal human femur as an Euler column may yield a more definitive evaluation of this analogy.

The use of synthetic femurs

Artificial longbone surrogates offer attractive advantages over human bone for biomedical research, such as low cost, no toxicity, easy storage, no decay with time, and standardized geometry from specimen to specimen. Intact synthetic femurs have previously demonstrated similar trends for axial versus torsional rigidity when compared with intact human cadaveric femurs.[6,33] They have also yielded similar cortical and cancellous screw pullout force and shear stress during screw extraction experiments relative to human cadaveric femurs.[29,30] These findings confirm the agreement that exists

between the human and synthetic femurs of the present study for the crush parameters measured and some fracture patterns observed. Even so, conflicting reports exist about whether the failure loads and patterns of intact specimens and surgical bone-implant constructs are different when using human versus synthetic longbone.[34–39] This divergence may be caused by the various test setups, applications, and longbone material properties used by investigators. There is a need to standardize test methods for proper interstudy comparison and adequate matching of geometric and material properties of human versus synthetic longbones.

Limitations

Despite the several drawbacks to this investigation outlined below, this is the first study to date that has quantified crush injury of any kind for the distal femoral condyles of intact human versus synthetic femurs.

Low speed load application (5 mm/min) was used to minimize viscoelastic effects on the results. Low speed force application (6 mm/min) was also used in a similar prior study.[24] A more realistic scenario would involve loads applied at higher speeds to simulate actual trauma from motor vehicle accidents, sports injuries, and falls. This would cause an increase in the crush stiffness, strength, and energy, since biological and polymeric materials have mechanical properties that are strain rate dependent.[10,15,40,41] However, the choice of a higher speed representing a specific injury mechanism, e.g. football tackle, slipping on ice, etc., would have made the results less generalizable to other injury mechanisms. Moreover, the advantage of low speed was that present results provide a lower bound value for the measurements.

The role of the patella was not simulated in the test setup, since only a flat plate load applicator was used. This was also done in a prior similar study.[24] This avoided the difficulties of fabricating an adjustable patellar geometry to accommodate varying geometries of human femurs. It may be important, however, to model the patella since it is commonly wedged in-between the condyles to produce inter-condylar fractures during 'dashboard' injuries in motor vehicle accidents.[5,23] Although all the failed synthetic femurs had a fracture line in-between the condyles through the intramedullary canal hole, less than half of present human femurs had unicondylar or bicondylar fracture lines.

Some muscle and soft tissue were present on the human femurs. No soft tissue was simulated on the synthetic femurs. It could be argued that the surrounding tissue would absorb some injury force through 'cushioning', which could reduce trauma to the underlying bone. However, this effect is likely to be quite small because the amount of soft tissue surrounding the distal condyles is minimal compared with the mid- and proximal-segments of the femur. A more substantial cushioning effect, however, has been reported when the axial load applicator itself has been padded to simulate different surfaces against which injury can occur.[23]

The metal plate used for load application did not have rotational freedom to automatically load both condyles equally. As described earlier, a metal plate and leveling gauge were used to ensure that the top of the condyles was perfectly horizontal, although this was no guarantee of equal condylar loading. This was done purposely, in part, so that the current setup would simulate the real-world scenario of 'dashboard injury' during a motor vehicle accident, in which the condyles are not necessarily equally loaded as the knee is impacted against a flat hard surface. Nonetheless, because this is a comparative study in which all specimens were loaded the same way, it is expected that the relative performance of human versus synthetic femurs would have been the same had a more optimal test setup been used.

Only left human femurs were tested. Similar results would be expected if right femurs had also been tested. Although a population group or individual might display a nominally different geometry from side-to-side for their lower limbs,[42] there is no statistical difference between the mechanical properties of the bone when comparing left versus right human femurs.[43] A previous study also demonstrated no left-versus-right difference in human cadaveric femurs concerning the simultaneous mechanical coupling of torsion and tension.[16]

Twelve of the 16 human femurs had normal bone quality. Although the data can help researchers better understand the nature of femoral bone injury in those with healthy bone, a deeper understanding of the behaviour of osteoporotic or osteopenic bone has not been gained. Consequently, poor bone quality would likely have yielded lower values.

Synthetic femurs had uniform size and bone density, thereby representing only one type of artificial femur. Changing cancellous bone density for these specimens may have altered the present results, since some of the current authors have shown that axial failure load, displacement, and energy at the femoral neck changes substantially with changes in cancellous bone density.[27]

There was relatively large interspecimen variation for human femurs with standard deviations ranging from 30% to 47% of the mean values, whereas synthetic femur standard deviations were somewhat smaller at 11% to 41% of the mean values (Table 2). Such variability is common for human bone. For example, axial and torsional stiffnesses for intact whole human femurs can vary by 3.3 and 3.2 times, respectively,[6] the standard deviation for cortical bone screw pullout stress can be 31% of the mean value,[29] and the standard deviation for cancellous bone screw pullout stress can be 91% of the mean value.[30]. Even so, current statistical comparisons demonstrated differences for human versus synthetic femurs for three of four outcome parameters. For an adequately powered study like the present investigation, the final statistical p value, rather than the size of the standard deviation, is the important factor to consider.

Finite element modelling and analysis were not performed to assess the stresses on the distal femur. Future researchers may wish to do so to gain a better understanding of the surface and internal stress distributions of the distal femur during axial injury. For example, the current investigators have employed computer modelling to look at the stress distribution of femurs implanted with joint replacement and fracture fixation devices, as well as femurs in an intact state.[6,14,44–48] Computational modelling is often particularly helpful in identifying areas of peak stress, i.e. areas of potential clinical failure. Since the present authors directly measured non-destructive and destructive parameters, finite element modelling was not needed to predict areas of potential failure in the distal femur. Moreover, computer modelling was beyond the present scope of the study, which was meant only to be experimental in nature.

Conclusions

The authors measured axial distal crush injury of the distal condyles of human and synthetic femurs. The two groups were statistically different in three of four measurement outcomes. The only correlation of any note was crush strength versus bone quality, as expressed in both sBMD and clinical T-score. Failure modes were mostly different for human versus synthetic specimens. This study showed that load application using a flat metal plate often cannot simulate the patellar wedging that causes type B or C clinical injury patterns in the distal human femur. This is the first study to have performed such an evaluation on human and synthetic femurs.

Funding

This research received no specific grant from any funding agency in the public, commercial, or not-for-profit sectors.

References

1. DeFrances CJ, Lucas CA, Buie VC, et al. 2006 national hospital discharge survey. *Natl Health Stat Report* 2008; 5: 1–20.
2. Martinet O, Cordey J, Harder Y, et al. The epidemiology of fractures of the distal femur. *Injury* 2000; 31(S3): C62–C63.
3. Crist BD, Della Rocca GJ and Murtha YM. Treatment of acute distal femur fractures. *Orthopedics* 2008; 31(7): 681.
4. Marsh JL, Slongo TF, Agel J, et al. Fracture and dislocation classification compendium – 2007: Orthopaedic Trauma Association classification, database and outcomes committee. *J Orthop Trauma* 2007; 21(10): S31–S133.
5. Elstrom JA, Virkus WW and Pankovich AM. (eds), *Handbook of fractures: 3rd edition*. New York, NY, USA: McGraw-Hill, 2006, pp.264–313.
6. Papini M, Zdero R, Schemitsch EH, et al. The biomechanics of human femurs in axial and torsional loading: comparison of finite element analysis, human cadaveric femurs, and synthetic femurs. *J Biomech Eng* 2007; 129(1): 12–19.
7. Cristofolini L, Viceconti M, Cappello A, et al. Mechanical validation of whole bone composite femur models. *J Biomech* 1996; 29(4): 525–535.
8. Martens M, Van Audekercke R, De Meester P, et al. The mechanical characteristics of the long bones of the lower extremity in torsional loading. *J Biomech* 1980; 13(8): 667–676.
9. Martens M, Van Audekercke R, De Meester P, et al. Mechanical behaviour of femoral bones in bending loading. *J Biomech* 1986; 19(6): 443–454.
10. Mather BS. Observations on the effects of static and impact loading on the human femur. *J Biomech* 1968; 1(4): 331–335.
11. Kuzyk P, Lobo J, Whelan D, et al. Biomechanical evaluation of extramedullary versus intramedullary fixation for reverse obliquity intertrochanteric fractures. *J Orthop Trauma* 2009; 23(1): 31–38.
12. Lever JP, Zdero R, Nousiainen MT, et al. The biomechanical analysis of three plating fixation systems for periprosthetic femoral fracture near the tip of a total hip arthroplasty. *J Orthop Surg Res* 2010; 5(45): 1–8.
13. McConnell A, Zdero R, Syed K, et al. The biomechanics of ipsilateral intertrochanteric and femoral shaft fractures: a comparison of 5 fracture fixation techniques. *J Orthop Trauma* 2008; 22(8): 517–524.
14. Zdero R, Bougherara H, Dubov A, et al. The effect of cortex thickness on intact femur biomechanics: a comparison of finite element analysis with synthetic femurs. *Proc IMechE, Part H: J Engineering in Medicine* 2010; 224(H7): 831–840.
15. Zdero R, Shah S, Mosli M, et al. The effect of load application rate on the biomechanics of synthetic femurs. *Proc IMechE, Part H: J Engineering in Medicine* 2010; 224(H4): 599–605.
16. Zdero R, McConnell AJ, Peskun C, et al. Biomechanical measurements of torsion–tension coupling in human cadaveric femurs. *J Biomech Eng* 2011; 133(1): 014501-1-6.
17. Marti A, Fankhauser C, Frenk A, et al. Biomechanical evaluation of the less invasive stabilization system for the internal fixation of distal femur fractures. *J Orthop Trauma* 2001; 15(7): 482–487.
18. Zlowodzki M, Williamson S, Cole PA, et al. Biomechanical evaluation of the less invasive stabilization system, angled blade plate, and retrograde intramedullary nail for the internal fixation of distal femur fractures. *J Orthop Trauma* 2004; 18(8): 494–502.
19. Zlowodzki M, Williamson S, Zardiackas LD, et al. Biomechanical evaluation of the less invasive stabilization system and the 95-degree angled blade plate for the internal fixation of distal femur fractures in human cadaveric bones with high bone mineral density. *J Trauma* 2006; 60(4): 836–840.
20. Higgins TF, Pittman G, Hines J, et al. Biomechanical analysis of distal femur fracture fixation: fixed-angle screw-plate construct versus condylar blade plate. *J Orthop Trauma* 2007; 21(1): 43–46.
21. Huiskes R and Van Rietbergen B. Biomechanics of bone. In: Mow VC and Huiskes R (eds) *Basic orthopaedic*

biomechanics and mechano-biology. 3rd ed. Philadelphia, PA: Lippincott Williams and Wilkins, 2005, pp.123–179.
22. Thompson I and Hench LL. Mechanical properties of bioactive glasses, glass-ceramics, and composites. *Proc IMechE, Part H: J Engineering in Medicine* 1998; 212: 127–136.
23. Viano DC and Stalnaker RL. Mechanisms of femoral fracture. *J Biomech* 1980; 13: 701–715.
24. Murray PJ, Damron TA, Green JK, et al. Contained femoral defects: biomechanical analysis of pin augmentation in Cement. *Clin Orthop Rel Res* 2004; 420: 251–256.
25. Warrington EK and Weiskrantz L. Amnesic syndrome: consolidation or retrieval? *Nature* 1970; 228: 628–630.
26. Cohen J. *Statistical power analysis for the behavioral sciences*. Revised edition. New York, USA: Academic Press, 1977.
27. Nicayenzi B, Shah S, Schemitsch EH, et al. The biomechanical effect of changes in cancellous bone density on femur behavior. *Proc IMechE, Part H: J Engineering in Medicine* 2011; 225(H11): 1050–1060.
28. Olsen M, Sellan M, Zdero R, et al. A biomechanical comparison of epiphyseal versus metaphyseal fixed conservative hip arthroplasty. *J Bone Joint Surg Am* 2011; 93(Suppl 2): 122–127.
29. Zdero R, Elfallah K, Olsen M, et al. Cortical screw purchase in synthetic and human femurs. *J Biomech Eng* 2009; 131(9); 094503-1-7.
30. Zdero R, Olsen, M, Bougherara H, et al. Cancellous bone screw purchase: a comparison of synthetic femurs, human femurs, and finite element analysis. *Proc. IMechE, Part H: J Engineering in Medicine* 2008; 222(H8): 1175–1183.
31. Norton RL. *Machine design: an integrated approach*. Upper Saddle River, NJ, USA: Prentice-Hall, 1996, pp.237–241.
32. Sawbones. http://www.sawbones.com/catalog/pdf/us_catalog.pdf (accessed 2 Nov 2011).
33. Heiner AD and Brown TD. Structural properties of an improved redesign of composite replicate femurs and tibias. *Trans 29th Soc Biomater* 2003; 26: 702.
34. Davis ET, Olsen M, Zdero R, et al. Femoral neck fracture following hip resurfacing: the effect of alignment of the femoral component *J Bone Joint Surg Br* 2008; 90(11): 1522–1527.
35. Dunlap JT, Chong ACM, Lucas GL, et al. Structural properties of a novel design of composite analogue humeri models. *Ann Biomed Eng* 2008; 36(11): 1922–1926.
36. Lescheid J, Zdero R, Shah S, et al. The biomechanics of locked plating for repairing proximal humerus fractures with or without medial cortical support. *J Trauma* 2010; 69(5), 1235–1242.
37. Lin J, Inoue N, Valdevit A, et al. Biomechanical comparison of antegrade and retrograde nailing of humeral shaft fracture. *Clin Orthop Rel Res* 1998; 351: 203–213.
38. Schopfer A, Hearn TC, Malisano L, et al. Comparison of torsional strength of humeral intramedullary nailing: a cadaveric study. *J Orthop Trauma* 1994; 8(5): 414–421.
39. Siffri PC, Peindl RD, Coley ER, et al. Biomechanical analysis of blade plate versus locking plate fixation for a proximal humerus fracture: comparison using cadaveric and synthetic humeri. *J Orthop Trauma* 2006; 20(8); 547–554.
40. Zdero R, Shah S, Mosli M, et al. The effect of the screw pull-out rate on cortical screw purchase in unreamed and reamed synthetic long bones. *Proc IMechE, Part H: J Engineering in Medicine* 2010; 224(H3): 503–513.
41. Zdero R and Schemitsch EH. The effect of screw pullout rate on screw purchase in synthetic cancellous bone. *J Biomech Eng* 2009; 131(2): 024501-1-5.
42. Auerbach BM and Ruff CB. Limb bone bilateral asymmetry: variability and commonality among modern humans. *J Hum Evol* 2006; 50(2): 203–218.
43. Banse X, Delloye C, Cornu O, et al. Comparative left-right mechanical testing of cancellous bone from normal femoral heads. *J Biomech* 1996; 29(10): 1247–1253.
44. Bougherara H, Zdero R, Mahboob Z, et al. H. The biomechanics of a validated finite element model of stress shielding in a novel hybrid total knee replacement. *Proc IMechE, Part H: J Engineering in Medicine* 2010; 224(10): 1209–1219.
45. Davis ET, Olsen M, Zdero R, et al. A biomechanical and finite element analysis of femoral neck notching during hip resurfacing. *J Biomech Engng* 2009; 131(4): 041002-1-8.
46. Bougherara H, Zdero R, Miric M, et al. The biomechanics of the T2 femoral nailing system: a comparison of synthetic femurs with finite element analysis. *Proc IMechE, Part H: J Engineering in Medicine* 2009; 223(H3): 303–314.
47. Shah S, Kim SYR, Dubov A, et al. The biomechanics of plate fixation of periprosthetic femoral fractures near the tip of a total hip implant: cables, screws, or both? *Proc IMechE, Part H: J Engineering in Medicine* 2011; 225(9): 845–856.
48. Dubov A, Kim SYR, Shah S, et al. The biomechanics of plate repair of periprosthetic femur fractures near the tip of a total hip implant: the effect of cable-screw position. *Proc IMechE, Part H: J Engineering in Medicine* 2011; 225(9): 857–865.

Appendix

Notation

p	statistical difference criterion
E	modulus of elasticity
F_{CR}	Euler column buckling force
H	Euler column height
I	area moment of inertia
N	number of specimens per test group
R^2	correlation coefficient
T	clinical score of bone quality
W_{AP}	anteroposterior femur condylar width
W_{ML}	mediolateral femur condylar width
δ	minimum difference between test groups that is clinically important and/or statistically detectable
μ	average value of measurement for each femur group
σ	total population standard deviation